Variability of Saharan Cyclone Tracks, I: Climatology Study

Abdulhaleem H. Labban
King Abdulaziz University
Adel M. Awad (awad_adel@yahoo.com)
King Abdulaziz University https://orcid.org/0000-0002-3314-8656

Research Article

Keywords: Saharan cyclone, Cyclone tracks, Cyclogenesis areas, Cyclolysis areas, Main cyclonic routes

Posted Date: November 3rd, 2021

DOI: https://doi.org/10.21203/rs.3.rs-940530/v1

Abstract

Objectively, Saharan cyclones have been detected for the period from 1967 to 2019 using mean sea level pressure (SLP); their tracks have been specified from nearest neighbor cyclonic positions and classified into long/short tracks depending on the area of influence of the cyclones. Additionally, the detected long tracks have been objectively classified into five main routes directed generally eastward, northeastward and northward, accounting for approximately 41.6%, 19.7% and 30.4% of the total long tracks, respectively.

Mainly for long tracks, three cyclogenesis areas, where more than 99% of cyclones are generated, were identified, with more than 61% generated in the Atlas region. Moreover, four far cyclolysis areas were identified, where approximately 74% of these cyclones terminated, with more than 66% of them terminating in the eastern study region. Furthermore, statistical analysis indicated that Saharan cyclones are commonly generated in the spring and summer, with ~35.3% and 46.3%, respectively. However, the highest numbers occur in spring in the northern Saharan and in summer in the southern Saharan, with ~49.1% and 57.7%, respectively.

Temporally, the monthly distribution indicates that most of the cyclones moving along the five main routes are generated in warm months, namely, May to August. Approximately 85% of these cyclones have a lifespan of three days, while only 1% span more than five days.

1- Introduction

The Saharan region is classified as a dominant global source of aeolian and mineral dust (Prospero et al. 2002; Washington et al. 2003), and large dust plumes are transported to the surrounding regions and beyond (see, e.g., Guerzoni and Chester 1996; Heintzenberg 2009; Muller et al. 2009). The atmospheric transport of mineral dust may play an important role in climate forcing by altering the radiation balance in the atmosphere through the processes of the scattering and absorption of radiation (Tegen et al., 1997; Haywood and Boucher, 2000; Harrison et al., 2001; Sokolik et al.,2001). Consequently, the climate of the Saharan region plays an important role in the dynamic characteristics of the global climate system through, for example, the radiative properties of the region and as a source of mineral dust. Based on simulations of climate change scenarios (Schubert et al. 1998; Leckebusch and Ulbrich 2004), a northward shift in cyclone tracks was found with warming climate state. Moreover, the intraseasonal and interannual variabilities in Saharan cyclogenesis have influenced the poleward transport of energy (Alpert et al. 1990a&b) and initiation of dust storms (Egger et al. 1995), which in turn have influenced the features of the Saharan climate.

Identifying the regional distribution of the generation, growth, translation, and decay of high- and low-pressure systems is of central importance for characterizing extratropical climates (Wernli and Schwierz 2006) and investigate climate change simulations from a synoptic perspective (e.g., Hall et al. 1994; Sinclair and Watterson 1999; Fyfe 2003; Raible and Blender 2004).

Specifying cyclone tracks can aid in determining the locations influenced by dust storms (Trigo et al. 2002), and variations in the mean tracks, caused either by anthropogenic factors or by long-term natural variability (Blender and Schubert 2000), have strong influences on regional climate. For example, southern Mediterranean cyclones appear as secondary lows of the large North African depression (Romero et al. 1999; Jans`a et al. 2001; Almazroui et al. 2017).

Over land during the warm season, strong sensible heating plays an important role in the genesis and preservation of cyclones, and the southward extension of cyclones deepens the upper troughs in the Lee Atlas (Campins et al. 2010). However, in the cold season (Thorncroft and Flocas 1997) show that the southward movement of the polar jet stream and its interaction with the subtropical jet can cause surface cyclogenesis in the Saharan area. In addition to the previously established factors that influence Saharan cyclogenesis, Lee cyclogenesis likely constitutes a main initiation mechanism and plays an important role in the growth, development and variability of Saharan lows (Egger et al. 1995).

This study specifies the generated Saharan cyclones and their tracks over the whole Saharan region and throughout the year considering all seasons, not only a specified season or area (Prezerakos 1985; Hannachi et al. 2011; Ammar et al. 2014), from 1967 to 2019, not for a short period or small area (Alpert et al. 1990b; Trigo et al. 1999 &2002; Maheras et al. 2001;); thus, a reliable view of Saharan cyclone variants can be obtained.

In this study, we determine the main sources, tracks and termination regions of Saharan cyclones and describe the internal structure of Saharan cyclones by studying the span time, characteristics of the sources and termination regions, and monthly/seasonal variabilities. Saharan cyclones are classified into long/short tracks, which represents the first step in studying regional climate or regional climate variability.

This paper is organized as follows. Section 2 describes the data and methodology. Section 3 presents and discusses the results of the statistical characteristics of the detected Saharan cyclones. The summary and conclusions are given in the final section.

2- Data And Methodology

Using the objective method developed by (Hannachi et al. 2011; Almazroui et al. 2015), generated cyclones and their tracks were objectively identified in the Saharan region, i.e., the area between longitudes 10° W-32.5° E and latitudes 17.5° N-32.5° N. The cyclone characteristics were identified based on the mean sea level pressure (SLP) data from the National Center for Environmental Prediction/National Center for Atmospheric Research (NCEP/NCAR) from 1967 to 2019. The data have a 6-hour temporal resolution and are based on a regular 2.5°×2.5° latitude-longitude grid (Kistler et al. 2001; Kalnay et al. 1996). The identified cyclones were used to classify the cyclogenesis, cyclolysis and affected areas in the study region.

As an initial step, the original low spatial resolutions of SLP data were transformed to a finer grid (0.5° × 0.5°) based on an established method (Pinto et al. 2005; Hannachi et al. 2011; Almazroui et al. 2015) to increase the availability of off-grid-identified cyclone centers and tracks. Then, briefly, the method described on (Hannachi et al. 2011; Almazroui et al. 2015), a cyclone center at a grid point was defined considering the following conditions:

- The SLP value is smaller than or equal to the value at each of the eight neighboring grid points.
- The pressure difference between the considered grid center and each of the neighboring eight grid points ranges from 0.8 to 3.8 hPa, as noted by Ziv et al. (2013).
- The SLP value is less than 1008.8 hPa, which is adequate to detect the initial stages of the development of Saharan cyclones and less than the value used by Bartholy et al. (2006) of 1012 hPa.

Furthermore, based on previous findings (Hannachi et al. 2011; Almazroui et al. 2015), the cyclone tracks were determined as follows:

- Around the first point representing a detected cyclone center, a box containing 20 fine grid points in all directions is used to search for a new track location, i.e., the next low-pressure center.
- After specifying the location of the next center, the previous step is repeated for this new location while considering the results at the previous point in the track.
- If no cyclone center is detected in the subsequent three time steps or the new center is beyond 50° E or 50° N, the track is terminated, and a new track search begins using a considered cyclone center in the Saharan region.

Some important classification steps were applied to the detected cyclonic tracks to specify the main area influenced by the Saharan cyclones.

1- Long/short classification: The detected cyclonic tracks were classified into either short or long-track groups. The short tracks correspond to cyclones that affected local areas and stayed within the areas where they were generated; i.e., the tracks have latitudinal ranges less than or equal to 5° and longitudinal ranges less than or equal to 10°. Only 5° of latitude is used to prevent the cyclone moving into a new climate region, because a short latitudinal distance can shift a cyclone from the Saharan region to the Mediterranean region, i.e. a different climate region; however, this shift does not appear if 10° of longitude is used. However, long tracks correspond to cyclones that greatly affect their generation areas and potentially other areas.

2- Cyclogenesis areas: In this study, only the main cyclogenesis areas are considered, i.e., the areas where most cyclones are generated.

3- Cyclolysis areas: In this study, only the main cyclolysis areas are considered, i.e. areas highly affected by the final positions (grid point) of cyclone tracks.

4- Affected areas: This term has not been previously defined but indicates areas that are highly affected at least once by cyclones.

To specify the main routes of long tracks, the route classification method used by (Hannachi et al. 2011; Almazroui et al. 2015; Almazroui and Awad 2016) was applied; briefly, the following two steps were used for classifying long tracks into the five main routes.

STEP 1: Specifying the key routes

i) Each cyclone track was divided into 6-hour segments to identify the track line between consecutive time steps over the cyclone Then, the slope, or angle from the north direction, of each segment was The slope angles ranges (i.e., the difference between the maximum and minimum angles of all slopes for each track were distributed into intervals, each spanning 20°.

ii) The interval that contained the maximum number of segments for all tracks was identified, and all tracks were then reassessed to determine which tracks belong to the maximum frequency These tracks were grouped into Filter A.
iii) Tracks belonging to Filter A were regrouped, and through identification, these tracks were found to have at least 70% of the same segment slopes (called the A1 subgroup). The latitude and longitude information (based on the percentage of similar segment was divided to create a 0.5^{o} lat/long grid, and for each crossing longitude/latitude, the latitudes/longitude of the available track segments were detected. Averaging all the corresponding latitude/longitude values provided all points for cluster A1. From the entire set of tracks, the tracks similar to those in cluster A1 with a correlation of at least $\geq 70\%$ and a latitudinal/longitudinal distance of $\leq 6°$ were assigned to cluster A1 and excluded from the next stage.
iv) Task iii was repeated to obtain cluster A2 with a target of 60% Tracks for cluster A2 were excluded from the next stage.
v) Task iii was repeated to obtain cluster A3 with a target of 50% Tracks for cluster A3 were excluded from the next stage.
vi) Tasks i-v were repeated with the next highest segment frequencies to obtain Filter B and cluster B1 (C1), cluster B2 (C2), and cluster B3 (C3).
vii) The nine clusters were classified based on similarity, which was determined by their intercorrelations based on tracks that overlap by at least $\geq 80\%$ and a latitudinal/longitudinal distance range of $\leq 2.5°$. Finally, only five high-frequency key routes were identified to classify the long tracks.

STEP 2: Specify the main routes: All tracks were classified into one of the five key routes based on the following two criteria: (a) the correlation between the track and the key route was $\geq 75\%$, and (b) the average latitudinal/longitudinal distance of each track was less than 400/600 km from the key route.

3- Results And Discussion

By applying the above method, approximately 5851 tracks were detected, and they were divided into 3221 (or 55.1% of the whole tracks) long tracks and 2630 (or 44.9%) short tracks; i.e., most of the generated cyclones had long tracks.

The seasonal distribution of the detected tracks, as shown in Table 1, indicates that approximately 296 tracks were detected in winter, with more than 55% being long tracks; in spring, approximately 1722 tracks (or 29.43 of the total tracks) were detected, and more than 66% were long tracks. Furthermore, 2912 tracks (or 49.77% of the total detected tracks) were observed in summer, with more than 51% being long tracks, and 921 tracks were identified in autumn, with 46.69% long tracks and 53.31% short tracks. This seasonal distribution suggested that most of the cyclone tracks were generated in summer and spring, with ratios of 49.77% and 29.43%, or a total of approximately 79.2% of all tracks; similar findings were noted in previous studies (Raible et al. 2008; Varga et al. 2014) of the cyclone center density over the Saharan region, which reaches a maximum in summer. However, the current results are opposite to those for the seasonal Mediterranean (the closed northern water area in the Sahara region) (intense) cyclone peak, which occurs in winter (HMSO 1962; Flaounas et al. 2013&2015), but the results from (Maheras et al. 2001; Trigo et al. 2002) for the western (not eastern) Mediterranean were compatible with the current results. The contradiction of these results with those of previous studies (Prezerakos 1985; Trigo et al. 1999; Maheras et al. 2001; Trigo et al. 2002) for Saharan depressions that reached their maximum frequency in spring and not in summer arose because the current results considered the whole Saharan region, not only the northwest African or the Atlas depressions, as studied in these works.

Table 1
Seasonal/total distribution of the classified long- and short-track Saharan cyclones detected. The percentage of the total number is given in parentheses.

Season/Class	Total	Long	Short
Winter	296 **(5.1%)**	163 **(5.1%)**	133 **(5.0%)**
Spring	1722 **(29.4%)**	1138 **(35.3%)**	584 **(22.2%)**
Summer	2912 **(49.8%)**	1490 **(46.3%)**	1422 **(54.1%)**
Autumn	921 **(15.7%)**	430 **(13.3%)**	491 **(18.7%)**
Total	5851	3221	2630

The annual track distribution (Figure 1-a) shows that approximately 58% of years, or 31 years, have fewer tracks than the annual average, that is 61 tracks/year, with the lowest numbers in 1992 and 1993 (47 tracks) and 2015 (39 tracks). The lowest number of tracks in 1992 agrees with tracks that influenced Turkey (Karaca et al. 2000), but the highest number during the widespread drought in 1989 (76 tracks) contrasted with their results (Karabulut 2015). Approximately 42% of years have a more track than the annual average, with the highest numbers of tracks (80) observed in 1980 and 2018, in contrast with the annual distribution of tracks that influenced Turkey (Karaca et al. 2000). Moreover, this annual distribution displayed a concave shape, with the highest values in the 1970s and the first decade of the

twenty-first century and lowest values in the 1980s-1990s. Additionally, approximately 47% of years had between 55 and 72 tracks per year, i.e., between the average and +/-10% of the average. Generally, the intersection period of the annual distribution of Saharan cyclones is similar to the annual winter distribution of mid-latitude but opposite to that of high-latitude cyclones in the North Atlantic (Wang et al. 2006).

The monthly distribution (Figure 1-b) indicated that from October (114 tracks) to March (248 tracks), the number of tracks was lower than the monthly track average (approximately 269 tracks/month); the lowest numbers of tracks were observed in December, November and January, with values of 18, 39 and 40, respectively. These results were consistent with the results of (Alpert et al. 1990b; Trigo et al. 1999) but in contrast with the monthly distribution of tracks that influenced Turkey (Karaca et al. 2000); this difference may have appeared because their study concentrated only on cyclones that reached Turkey.

In contrast, the months from April to September had the highest track numbers, with more tracks than the monthly average; the month with the most tracks was July, with 531 tracks, or approximately two times the monthly average (269 tracks), then coming May with 482 tracks. Of these months, September had the fewest tracks at 275, or approximately the monthly average. The results from (Trigo et al. 1999) were inconsistent with the current results, where the maximum number of cyclones occurred in May and was not high in July; this difference may be explained by the fact that their results depended on cyclones generated in only a small area, namely, the Atlas region.

3-1 Cyclogenesis areas

The spatial distribution of the Saharan cyclone regions, as shown in Figure 2-a, includes three main generation areas: the Atlas area (the area between 10° W-10° E and 15° N to 32.5° N, labeled “ATLAS” in the figure), the South Saharan area (the area between 10° E-37.5° E and 15° N to 22.5° N, labeled “STHSH” in the figure), and the North Saharan area (the area between 10° E-37.5° E and 22.5° N to 35.0° N, labeled “NTHSH” in the figure). These cyclogenesis areas were classified as main Saharan dust sources (Prospero et al. 2002; Israelevich et al. 2002) or as main high-frequency cyclone regions (Wernli and Schwierz 2006).

Approximately 61.87% of the long Saharan cyclone tracks (or 1993 cyclones) were generated in the Atlas area, and approximately 31.08% (or 1001 cyclones) and 7.05% (or 227 cyclones) were generated in the southern and northern Saharan areas, respectively (Table 2). This result is similar to the findings of Raible et al. (2008) for Northern Hemisphere (NH) cyclone centers and Trigo et al. (2002) for Mediterranean basin cyclone sources. Additionally, the results indicate that the lowest number of long-track Saharan cyclones is generated in the northern Saharan area north of 22.5° N, while the Atlas area, which is classified as the primary source of dust for the Mediterranean region (Alpert et al. 1990-a&b; Israelevich et al. 2002; Hannachi et al. 2011) and is responsible for generating a low-level shallow vortex (Horvath et al. 2006b), is associated with the highest number of generated long-track Saharan cyclones.

Table 2
Seasonal/total numbers of Saharan cyclones generated in the main cyclogenesis areas

Areas/Season	Winter	Spring	Summer	Autumn	Total
Atlas (ATLAS)	84	717	949	243	1993
South Sahara (STHSH)	50	290	491	170	1001
North Sahara (NTHSH)	29	131	51	16	227

The seasonal distribution of long tracks (Table 2) indicated the corresponding cyclones generated in the Atlas area accounted for 84 (or 4.21%), 717 (or 35.98%), 949 (47.62%) and 243 (or 12.19%) of all cyclones in the winter, spring, summer and autumn seasons, respectively. These seasonal distributions suggest that most of the cyclones in this area are generated in summer and spring (or 83.6% of the cyclones generated in the two seasons), while the lowest number of cyclones is generated in winter. Of the south-Saharan cyclones (Table 2), the distribution of the generated tracks indicates that 78.02% of cyclones occurred in spring and summer, while 5.00% of cyclones occurred in winter, an increase over the corresponding value in the Atlas area. Of the north-Saharan cyclones, as shown in Table 2, the distribution of the generated tracks suggests that 57.71% of cyclones occurred in spring, and only 7.05% occurred in autumn. Additionally, the ratio of the number of cyclones generated in the northern Sahara area in winter reached more than 56% of that in summer (twenty-nine winter cyclones compared to 51 summer cyclones).

3-2 Cyclolysis areas

The generated cyclones terminate in four main areas, as shown in Figure 2-b: the North African area, Mediterranean area, Arabian Peninsula and Red Sea area and eastern area. Approximately 2393 cyclones (74.29% from total generated cyclones) terminated in these four regions, and approximately 828 cyclones (or 25.71%) were not classified in any one of these areas (Table 3).

Table 3
Seasonal/total numbers of Saharan cyclone tracks that terminate in the main cyclolysis areas

Area/Season	Winter	Spring	Summer	Autumn	Total
North Africa (NRTREG)	9	149	196	29	383
Mediterranean (MEDREG)	48	189	124	58	419
AP and Red Sea (APSREG)	13	188	261	118	580
Eastern Area (ESTREG)	67	407	423	114	1011

The North African area (the area from 10° E to 35° E and from 22.5° N to 32.5° N, labeled “NRTREG” in Figure 2-b) was influenced by 383 cyclones (11.89% of the long cyclonic tracks, or 16.01% of the tracks

classified as associated with cyclolysis regions), including 9 (or 2.29%), 149 (or 38.90%), 196 (or 51.17%) and 29 (or 7.57%) in winter, spring, summer and autumn, respectively, as shown in Table 3.

The Mediterranean area (the area from 10° E to 37.5° E and from 32.5° N to 45° N, labeled “MEDREG” in Figure 2-b) was influenced by 419 cyclones (13.01% of the long tracks, or 17.51% of the tracks classified as associated with cyclolysis tracks), as shown in Table 3. This area was classified as a cyclone center by the NH (Raible et al. 2008) and was considered a generation area for eastern Mediterranean cyclones/rain (Alpert et al. 1990a&b; Kahanaet al. 2002; Rubin et al. 2007). Any discrepancies among results are potentially because the authors considered the existence of cyclones but did not consider cyclonic tracking. These cyclonic tracks include a maximum of 189 (or 45.11%) in spring (Table 3) and a minimum of 48 (11.46%) in winter (Table 3). The maximum number in this region was found in spring, not in summer, as in the North African area, although winter was the season with the fewest cyclones in both areas.

The Arabian Peninsula and Red Sea area (the area from 35° E to 57.5° E and from 15° N to 32.5° N, labeled “ARSREG” in Figure 2-b) was influenced by 580 cyclones (18.01% of the long-track cyclones, or 24.24% of the tracks classified as cyclolysis tracks), as shown in Table 3, with a maximum number of 261 cyclones in summer (or 45.0% of the area cyclones) and a minimum number of 13 cyclones in winter (or 2.24% of the area cyclones). Additionally, 306 cyclones formed in spring and autumn (or 32.41% and 20.34% in spring and autumn, respectively). This area was previously classified as a generation area for Mediterranean cyclones (Alpert et al. 1990a&b) because cyclones were detected in the area, but the tracks from the initial sources were not considered.

The Eastern area (the area from 37.5° E to 60° E and from 32.5° N to 50° N, labeled “ESTREG” in Figure 2-b) was influenced by 1011 cyclones (31.39% of the long-track cyclones, or 42.25% of the tracks classified as being associated with cyclolysis regions), as shown in Table 3. However, this area, especially around the Black and Caspian Seas, was considered a generation region for the Middle East (Alpert et al. 1990a&b) or an active cyclonic region linked with synoptic systems over Europe and the Mediterranean (Trigo et al. 2002). A highly seasonal distribution (Table 3) was found, with 423 cyclones (or 41.84% of the area cyclones) in summer and 407 cyclones (or 40.26% of the area cyclones) in spring; the minimum number of 67 cyclones was found in winter (6.63% of all cyclones in the area). This distribution indicated that more than 82% of the cyclones in the eastern area occur in spring and summer and only 11.3% occur in autumn.

3-3 Contributions of cyclogenesis in cyclolysis areas

The Atlas area was where 1261 (or 52.7%) of the cyclone tracks that reached the main cyclolysis areas (Table 4) formed, while the South Sahara and North Sahara areas were where 920 (or 38.4%) and 212 (or 8.9%) of these cyclones originated, respectively.

Table 4
Numbers of Saharan cyclones that move from cyclogenesis areas to cyclolysis areas

Cyclogenesis /Cyclolysis	Mediterranean (MEDREG)	North Africa (NRTREG)	AP and Red Sea (APSREG)	Eastern Region (ESTREG)
Atlas (ATLAS)	299	293	213	456
South Sahara (STHSH)	71	87	350	412
North Sahara (NTHSH)	49	3	17	143

In detail, Table 4 shows that 456 cyclones (or 45.1%) formed in the Atlas area and that 412 cyclones (or 40.8%) formed in the South Sahara area and moved to the eastern area, while only 143 cyclones (or 14.1%) formed in the North Sahara area. Most of the cyclones, approximately 299 (or 71.4%) and 293 (or 76.5%), that were generated in the Atlas area reached the Mediterranean and North African areas, respectively. Additionally, few cyclones from the Atlas, South Sahara and North Sahara areas, or 213 (or 10.69% from Atlas-generated cyclones), 71 (or 7.1% from South Sahara-generated cyclones) and 3 (or 1.32% from North Sahara-generated cyclones), reached the Arabian Peninsula and Red Sea area, Mediterranean and North African areas, respectively.

3-4 Affected regions

The most affected areas, i.e., the area influenced at least one time by any tracks, were identified based on long tracks, and four regions were highly influenced by Saharan cyclones (Figure 2-c): the South Sahara (labeled STHEF in the figure), North Sahara (labeled NRTEF in the figure), Mediterranean (labeled METEF in the figure) and Arabian Peninsula (labeled ARPEF in the figure) regions.

The STHEF region (the area from 00° E to 35° E and from 15° N to 23° N in Figure 2-c) was affected by 2076 cyclones (or approximately 64.45% of long-track cyclones), as shown in Table 5, and these cyclones were divided into 61 cyclones (or 2.94% of the cyclones that affected this region), 615 cyclones (or 29.62%), 1100 cyclones (or 52.99%) and 300 cyclones (or 14.45%) in winter, spring, summer and autumn, respectively.

Table 5
The seasonal/total numbers of cyclones that affect different regions

Area	South Area	Medit. Area	North Area	AP Area
Winter	61	103	98	21
Spring	615	485	611	252
Summer	1100	446	529	274
Autumn	300	153	171	85
Total	2076	1187	1409	632

The NRTEF region (the area from 00° E to17.5° E and from 24° N to 32.5° N in Figure 2-c) was affected by 1409 cyclones (or 43.74% of long-track cyclones), as shown in Table 5; this was the second most affected region by Saharan cyclones after the STHEF region. The seasonal effect in this region was highest in spring, with 611 cyclones, or 43.36% of the cyclones that affected the region, followed by 529 cyclones (or 37.54%) in summer.

The MEDEF region (the area from 20° E to 40° E and from 30° N to 37.5° N in Figure 2-c) was affected by 1187 cyclones (or 36.85% of the long-track cyclones), as shown in Table 5. The highest numbers of cyclones occurred in spring and summer, with 485 cyclones (or 40.86% of the cyclones that affected the region) and 446 cyclones (or 37.57%), respectively. However, the MEDEF region was weakly affected in winter and autumn, with 103 (or 8.68%) and 153 (or 12.89%) cyclones, respectively.

The ARPEF region (the area from 40° E to 50° E and from 25° N to 32.5° N in Figure 2-c) was the least affected area (Table 5); notably, only 632 cyclones (or 19.62% of the long-track cyclones) were observed in this area. Most of the cyclones were generated in summer and spring, with 274 cyclones (or 43.35%) and 252 cyclones (or 39.84%) in these seasons, respectively; thus, approximately 83.19% of all cyclones that affected the area occurred in these seasons.

3-5 Main routes

3-5-1 General description of main routes

By applying the route conditions, more than 90% of the long tracks were classified into five main routes (Table 6).

Table 6
Seasonal/total numbers (ratio, with respect to the total number of tracks along the route) of tracks for main routes

Route/Num.	South Sahara Route	North Sahara Route	Eastern Mediterranean Route	Northeast Egypt Route	Northern Route
Winter (**Ratio**)	11 (**1.18%**)	26 (**6.97%**)	29 (**5.81%**)	4 (**2.94%**)	81 (**8.27%**)
Spring (**Ratio**)	238 (**25.43%**)	236 (**63.27%**)	171 (**34.27%**)	62 (**45.59%**)	331 (**33.78%**)
Summer (**Ratio**)	535 (**57.16%**)	82 (**21.98%**)	224 (**44.89%**)	62 (**45.59%**)	435 (**44.39%**)
Autumn (**Ratio**)	152 (**16.24%**)	29 (**7.77%**)	75 (**15.03%**)	8 (**5.88%**)	133 (**13.57%**)
Total Num. (**Ratio**)	936 (**29.06%**)	373 (**11.58%**)	499 (**15.49%**)	136 (**4.22%**)	980 (**30.43%**)

The first route (or the South Sahara route) passes directly eastward over Sahara and northeast over the Arabian Peninsula (AP) (Figure 3-a); this route encompassed 936 tracks, or 29.06% of all long tracks (Table 6). This route was noted for spring by (Alpert et al. 1990b).

The second route (or North Sahara route) passes directly eastward over northern Africa and the south Mediterranean, and some of the corresponding tracks are directed southeastward over the northern AP (Figure 3-b). This route encompasses 373 tracks, or 11.58% of all long tracks (Table 6), and includes the area known as the Saharan depression or Khamasin depression (Tantawy 1964; Alpert and Ziv 1989) or the Saharan spring cyclones track (Alpert et al. 1990a&b).

The third route (or eastern Mediterranean route) passes generally northeast over Sahara and east/northeast over the Mediterranean and Middle East, and only a few tracks pass southeast over the Arabian Gulf (Figure 3-c). This route encompasses 499 tracks, or 15.49% of all long tracks, as shown in Table 6. This route is considered one of three main winter NH storm paths (Wernli and Schwierz 2006), or one of the four main passes that influence Turkey (Karaca et al. 2000). Both the HMSO (1962) and Alpert and Ziv (1989) suggested that this route in spring contributes to approximately 43% of the North African cyclones that reach the eastern coast of the Mediterranean.

The fourth route (or the northeast Egypt route) passes northeastward over Egypt and the Middle East and southeast over the region around the Arabian Gulf (Figure 3-d). This route encompasses 136 tracks, or 4.22% of all long tracks (Table 6). This route was mentioned by (Alpert and Ziv 1989; Awad and Mashat 2014) as a track for African dust.

The fifth route (or northern route) generally passes directly northward or near northward (Figure 3-e) and encompasses 980 tracks, or approximately 30.43% of all long tracks (Table 6). The cyclones from this route were considered as the main Saharan cyclones influenced Mediterranean (HMSO 1962; Prezerakos 1985; Prezerakos et al. 1990; Thorncroft and Flocas 1997; Horvath et al. 2006a&b; Bou Karam et al. 2010).

Generally, more than 31.29% of annual Saharan cyclones influence the eastern Mediterranean, the results are usually consistent with those of the HMSO (1962), showing that 58% of the cyclones that enter the Mediterranean region and 34.5% of cyclones that enter the Red Sea region originate from the Saharan region (Romem et al. 2007), if the influence of tracks that reach the whole Mediterranean and Red Sea regions at least one time is considered.

3-5-2 Seasonal and monthly variations in the main routes and their lifespans

The total monthly distribution of classified tracks, as shown in Figure 4-a, displays two high numbers of tracks, one in August, with 485 tracks, or 16.59% of the classified tracks, and the other in May, with 431 tracks, or 14.74% of the classified tracks. Furthermore, the lowest numbers of tracks were observed in November, December and January, with 34, 16 and 34 long classified tracks, accounting for less than 1.2% of classified tracks in each month. This situation contrasts with the monthly distribution of Mediterranean cyclones (the water area northern Sahara), where for example Alpert and Ziv (1989) suggested that the low numbers of cyclones in warm months was explained by the dominance of the subtropical high in warm months.

In particular, along the South Sahara route, RT1 in Figure 4-b, no tracks were observed in December or January, and the highest number of tracks occurred in July, with 217, or 23.18% of the tracks along that route.

December, with one track, was the month with the fewest tracks along the North Sahara route, RT2 as shown in Figure 4-b. The highest number of tracks occurred in April, with 96 tracks, or 25.74% of the tracks along that route, as shown in Table 6. This high number was explained (Elfandy 1940; Alpert and Ziv 1989) by the thermal gradient between the cold African continent and the warm Mediterranean water.

Generally, the seasonal distribution of route tracks (Table 6) suggests that the lowest number of tracks occurs in winter, while spring had the highest numbers for North Sahara and the eastern Mediterranean and most tracks occurred in summer along other routes.

The lifespan distribution indicates that more than 66% of tracks along the South Sahara route have lifespans between two and three days, as shown by RT1 in Figure 4-c; only approximately 16% of tracks have lifespans longer than three days, and approximately 17% of tracks have lifespans of one day or less.

For the North Sahara route, RT2 in Figure 4-c, more than 63% of tracks have lifespans between two and four days, more than 20% of tracks have lifespans of one day or less, and more than 16% of tracks have lifespans between four and 7 days.

Approximately 41% of the tracks along the Eastern Mediterranean route, RT3 in Figure 4-c, have lifespans of one day or less, more than 46% of tracks have a lifespan between two and three days, and only approximately 12% of tracks have a lifespan between four and seven days.

Most of the tracks, approximately 76%, along the northeast Egypt route, RT4 in Figure 4-c, have lifespans between two and four days, 18% of tracks have a lifespan of a day or less, and only 5% of tracks have lifespans of 5 to 6 days.

On the northern route, RT5 in Figure 4-c, more than 79% of tracks have a lifespan of two days, and more than 20% of tracks have a lifespan between three and six days.

Generally, previous results indicated that approximately 85% of tracks have lifespans of less than 3 days; notably, the typical lifespan of extratropical cyclone tracks is less than 2 days (Nielsen and Dole 1992; Trigo et al. 1999; Hanson et al. 2004). Moreover, the results show that less than 13% of the cyclone tracks have lifespans of greater than three days to five days, and only approximately 1% of route tracks have lifespans longer than five days. These results are consistent with the findings of Hannachi et al. (2011) for spring Saharan cyclones; additionally, according to a classification used in a study by (Raible et al. 2008), only approximately 14% of cyclones that have lifespan greater than three days can be classified as strong cyclones.

Furthermore, the longest lifespan for easterly routes (South/North Sahara) is nine days, and the lifespan of northerly routes (Northern and Northeast Mediterranean/Egypt) is shorter at six days.

3-5-3 Cyclogenesis and cyclolysis regions for main routes

The main area of cyclogenesis for the South Sahara route, as shown in Figure 5-a, delimited from 15^{o} N to 20^{o} N and distributed in three regions, namely, those between 5^{o} W and 7.5^{o} E, 10^{o} E and 22.5^{o} E, and 27.5^{o} E and 32.5^{o}E, were the sources of 323, 277 and 127 tracks (or 34.51%, 29.59% and 13.57% of the total tracks along the route), respectively. The cyclolysis areas were concentrated in four regions (Figure 5-b): local areas over Chad between 17.5°E and 22.5° E and three water areas over the Red Sea, around the Arabian Gulf and around the Caspian Sea.

The main cyclogenesis area for the North Sahara route, as shown in Figure 5-c, is the Atlas region, which was the source of 246 tracks (or 65.95% of the total tracks along the route), and some sparse areas in northern Africa contributing to the formation of 79 cyclone tracks (or 21.18% of the total tracks along the route). The local cyclolysis area (Figure 5-d) is located over the Sirte region in Libya, and the main termination area is the area around the Caspian Sea; in addition, less concentrated cyclolysis areas can be observed over Iraq and the Arabian Gulf. The Caspian Sea was previously mentioned as a cyclolysis area for western Saharan cyclones in spring (Hannachi et al. 2011). On the other hand, the area around

the Black and Caspian Seas was considered a cyclonic center by (Alpert et al. 1990a; Maheras et al. 2001; Campins et al. 2010), which authors not considered the tracks on their consideration.

For the eastern Mediterranean route, as shown in Figure 5-e, the southern Atlas region and the zone from 15° N to 20° N and 2.5°E to 20° E represent the main cyclogenesis areas, with109 tracks and 199 tracks (or 21.84% and 39.88% from total tracks of the route), respectively, forming in each area. The three main cyclolysis areas for this route (Figure 5-f) include the eastern Mediterranean, Black Sea, and Caspian Sea, with a less notable area over the Arabian Gulf. The Black Sea was previously mentioned as a cyclolysis area for Mediterranean cyclones (Trigo 2006; Romem et al. 2007), or for western Saharan cyclones in spring (Hannachi et al. 2011).

Generally, the Atlas region appeared as the source of the most cyclones that influenced the Mediterranean region, as previously indicated by (Alpert et al. 1990a&b; Hannachi et al. 2011)

Northern Sudan is the main cyclogenesis area for the Northeast Egypt route (Figure 5-g), and 64 cyclone tracks (or 47.06% of the total tracks along the route) formed there; Chad is a less frequent cyclogenesis area, with 43 associated tracks (or 31.62% of the total tracks along the route). Two cyclolysis areas for this route (Figure 5-h) are dense, and they are located near the Caspian Sea, while less frequent cyclolysis areas are located over the Arabian Gulf.

The cyclogenesis areas for the northern route (Figure 5-j) are the Atlas region and the area between 15° N and 20° N and between 2.5° E and 32.5° E; notably, 372 tracks and 348 tracks (or 37.96% and 35.51% of the total tracks along the route), respectively, originated in these areas. The Atlas contribution is comparable to the value of 46% proposed by Egger et al. (1995) for cyclones that originate in the Atlas region and travel along routes to the Mediterranean. The main cyclolysis area for this route, as shown in Figure 5-k, is located near southeastern Libya and Algeria. Furthermore, less frequent cyclolysis areas are located over the Mediterranean, the Adriatic Sea, the eastern Mediterranean, Iraq, Turkey and the Black Sea, as mentioned above (Maheras et al. 2001; Romem et al. 2007). Considering only the Atlas region, all (Prezerakos 1985; Prezerakos et al. 1990) were considered it as a source of Saharan cyclones influenced south Balkans area.

4- Summary And Conclusions

The climatology of the Saharan region cyclone tracks (routes) is objectively assessed (classified) and discussed in this paper. The study focuses on the cyclogenesis areas over the Saharan region (10° W-32.5° E and 17.5° N-32.5° N) over the whole year during the 1967-2019 period using 6-hour sea level pressure reanalysis data derived from the NCEP/NCAR dataset. Additionally, the cyclogenesis/cyclolysis areas of the detected Saharan cyclones are determined, and the contributions of main cyclogenesis areas to the main cyclolysis areas are statically assessed. Furthermore, the main routes of more than 90% of the long-track cyclones are classified and described. The main results are as follows.

1. Most of the detected tracks (55.1%) were long tracks, and they affected regions far from the main Saharan sources. The highest percentages of detected long tracks were found in spring and summer, and these tracks accounted for more than 81% of all long tracks.
2. In approximately 26% of the studied years, of 14 years, the number of long cyclone tracks was greater than the average number of cyclone tracks plus 10%. Furthermore, the annual distribution of cyclone tracks displays a concave shape with valley in the 1980s-1990s.
3. The monthly distribution of cyclone tracks demonstrated that the number of cyclone tracks increased in warm months, reached a maximum in July, and decreased in cold months, with a minimum in December.
4. The affected region results indicated that most of the Saharan cyclones pass through Sahara, where approximately 43.74% of the long cyclone tracks pass through the northern and southern Saharan regions. However, only approximately 19.62% of the long cyclone tracks pass through the Mediterranean and Arabian Peninsula regions.
5. The cyclogenesis analysis of Saharan cyclones indicated that the Atlas region is the main area for Saharan cyclone generation. Moreover, temporal, the results show that most North Saharan cyclones occur in spring, and most Atlas and South Saharan cyclones occur in summer.
6. The distribution of the cyclolysis areas indicated that more than 74% of the long tracks terminate in four cyclolysis regions. Additionally, more than 49% of the long-track Saharan cyclones (or more than 66% of cyclones from the cyclogenesis areas) reach the Arabian-Red Sea and eastern regions. Moreover, approximately 42% and 39% of these cyclones were generated in summer and spring, respectively (or 81% for both seasons), and only 5.7% were generated in winter.
7. The contributions of the main cyclogenesis regions to cyclolysis areas indicated that the majority of cyclones from the main cyclogenesis regions reached the eastern region. Additionally, few cyclones from the Atlas region, the South Sahara region and the North Sahara region reached the Arabian-Red Sea, the Mediterranean region and the eastern region, respectively. Additionally, the contributions of the cyclogenesis regions indicate that most of the cyclones that reach the Arabian-Red Sea region originate in the South Sahara region, and most of the cyclones that reach the Mediterranean and North African regions originate in the Atlas region. Comparable numbers of cyclones from the Atlas (approximately 45.1%) and South Sahara (approximately 40.8%) regions reach the eastern region.
8. Five main routes were classified from the detected long-track cyclones. Only approximately 9.22% of long tracks are not classified into one of these five main routes.
9. The direction of the main routes indicated that approximately 40.64% of the long tracks pass eastward and over South or North Sahara. Moreover, approximately 19.71% of the long tracks pass northeastward over the Mediterranean or Egypt, and more than 30% of the long tracks pass directly northward or nearly northward across the Sahara region.
10. The monthly distribution of classified routes indicated that most long-track cyclones occur in August and May, with the fewest number occurring from November to January. Nevertheless, for the easterly

routes (i.e., South and North Sahara routes), the highest numbers occurred in July for the South Sahara route and in April for the North Sahara route.

11. The lifespan of routes indicated that approximately 85% of tracks have a lifespan of approximately 3 days, and less than 13% of the cyclonic tracks have lifespans of more than three days to five days; only approximately 1% of route tracks have lifespans longer than five days.

Declarations

Acknowledgments

The authors are grateful to King Abdulaziz University for providing the facilities and logistical needs for this study. The authors also acknowledge NASA and the NCEP/NCAR for providing the meteorological data through their websites.

Competing interests: The authors declare no competing interests

References

1. Almazroui M, Awad AM, Islam MN, Al-Khalaf AK (2015) A climatological study: wet season cyclone tracks in the East Mediterranean region. Theor Appl Climatol 120:351–365. doi:10.1007/s00704-014-1178-z.
2. Almazroui M, Awad AM (2016) Synoptic regimes associated with the eastern Mediterranean wet season cyclone tracks. Atmos Res 180: 92–118.
3. Almazroui M, Awad AM, Nazrul Islam M (2017) Characteristics of the internal and external sources of the Mediterranean synoptic cyclones for the period 1956–2013. Theor Appl Climatol 133:811–827. https ://doi.org/10.1007/s0070 4-017-2218-2.
4. Alpert P, Ziv B (1989) The Sharav Cyclone: Observations and some theoretical considerations. J Geophys Res 94:18495–18514
5. Alpert P, Neeman BU, Shay-El Y (1990a) Climatological Analysis of Mediterranean Cyclones Using ECMWF Data. Tellus 42:65–77
6. Alpert P, Neeman BU, Shay-El Y (1990b) Intermonthly variability of cyclone tracks in the Mediterranean. J Climate 3(12):1474–1478.
7. Ammar, K., El-Metwally, M., Almazroui, M. et al. A climatological analysis of Saharan cyclones. Clim Dyn 43, 483–501 (2014). https://doi.org/10.1007/s00382-013-2025-0.
8. Awad, A.M. and Mashat, A.S. (2014) Synoptic features associated with dust transition processes from North Africa to Asia. Arabian Journal of Geosciences, 7(6), 2451–2467. https://doi.org/10.1007/s12517-013-0923-4.

9. Blender, R., and M. Schubert, 2000: Cyclone tracking in different spatial and temporal resolutions. Mon. Wea. Rev., 128, 377–384.
10. Bou Karam, D., Flamant, C., Cuesta, J., Pelon, J., Williams, E., 2010. Dust emission and transport associated with a Saharan depression: the February 2007 case. J. Geophys. Res. https://doi.org/10.1029/2009JD012390.
11. Campins J, Genoves A, Picornell MA, Jansa A (2010) Climatology of Mediterranean cyclones using the ERA-40 dataset. Int J Climatol 31:1596–1614
12. Egger J, Alpert P, Tafferner A, Ziv B (1995) Numerical experiments on the genesis of Sharav cyclones: idealized simulations. Tellus A 47(2): 162–174. doi:10.1034/j.1600-0870.1995.t01-1-00002.x
13. Elfandy, M. G., The formation of depressions of the Khamsin type, Q. J. R. Meteorol. Soc., 66, 325-335, 1940.
14. Flaounas E, Drobinski P, Bastin S (2013) Dynamical dowscaling of IPSL-CM5 CMIP5 historical simulations over the Mediterranean: benefits on the representation of regional surface winds and cyclogenesis. Clim Dyn 40:2497–2513. doi:10.1007/s00382-012-1606-7
15. Flaounas, E., S. Raveh-Rubin, H. Wernli, P. Drobinski, and S. Bastin (2015), The dynamical structure of intense Mediterranean cyclones, Clim. Dyn., 44, 2411–2427.
16. Fyfe, J. C., 2003: Extratropical Southern Hemisphere cyclones: Harbingers of climate change? J. Climate, 16, 2802–2805.
17. Hall, N. M. J., B. J. Hoskins, P. J. Valdes, and C. A. Senior, 1994: Storm tracks in a high-resolution GCM with doubled carbon dioxide. Quart. J. Roy. Meteor. Soc., 120, 1209–1230.
18. Hannachi A, Awad A, Ammar K (2011) Climatology and classification of Spring Saharan cyclone tracks. Clim Dyn 37:473–491.
19. Hanson, C. E., J. P. Palutikof, and T. D. Davies, 2004: Objective cyclone climatologies of the North Atlantic—A comparison between ECMWF and NCEP reanalyses. Climate Dyn., 22, 757–769.
20. Harrison, S. P., K. E. Kohfeld, C. Roelandt, and T. Claquin, The role of dust in climate changes today, at the Last Glacial Maximum and in the future, Earth Sci. Rev., 54, 43–80, 2001.
21. Haywood, J., and O. Boucher, Estimates of the direct and indirect radiative forcing due to tropospheric aerosols, Rev. Geophys., 38, 513–543, 2000.
22. HMSO (1962) Weather in the Mediterranean I: General Meteorology. 2nd ed., Her Majesty's Stationery Office, 362 p.
23. Horvath K, Fita L, Romero R, Ivancan-Picek B (2006-a) A numerical study of the first phase of a deep Mediterranean cyclone: cyclogenesis in the lee of the Atlas Mountains. Meteorol Zeitsch 15(2):133–146
24. Horvath K, Fita L, Romero R, Ivancan-Picek B, Sriperski I (2006-b) Cyclogenesis in the lee of the Atlas mountains: a factor separation numerical study. Adv Geosci 7:327–331.
25. Israelevich, P.L., Levin, Z., Joseph, J.H., Ganor, E., 2002. Desert aerosol transport in the Mediterranean region as inferred from the TOMS aerosol index. J. Geophys. Res. 107 (D21), 4572.

doi:10.1029/2001JD002011.

26. Kahana, R., B. Ziv, Y. Enzel, and U. Dayan, 2002: Synoptic climatology of major floods in the Negev Desert, Israel. Int. J. Climatol., 22, 867–882.
27. Kalnay E, Kanamitsu M, Kistler R, Collins W, Deaven D, Gandin L ,IridellM, Saha S, White G, WoollenJ,Zhu Y ,Chelliah M, Ebisuzaki W, Higgins W ,JanowiakJ,Mo KC, Ropolewski C, Wang J, Leetma A, Reynolds R, Jenne R, Joseph D (1996) The NCEP/NCAR 40-year Reanalysis project. Bull Am Meteorol Soc 77:437–471.
28. Karabulut, M. (2015). Drought analysis in Antakya-Kahramanmaraş Graben, Turkey. Journal of Arid Land, 7(6), 741-754
29. Karaca M, Deniz A, Tayanc¸M (2000) Cyclone track variability over Turkey in association with regional climate. Int J Climatol 20: 1225–1236.
30. Kistler R, Collins W, Saha S, White G, Woollen J, Kalnay E, Chelliah M, Ebisuzaki W, Kanamitsu M, Kousky V, vandenDool H, Jenne R, Fiorino M (2001) The NCEP/NCAR 50-year Reanalyses: Monthly CD-ROM and documentation.Bull Am Meteorol Soc 82:247–267
31. Leckebusch, G. C., and U. Ulbrich, 2004: On the relationship between cyclones and extreme windstorm events over Europe under climate change. Global Planet. Change, 44, 181–193.
32. Maheras P., H.A. Flocas, I. Patrikas, Chr. Anagnostopoulou, 2001: A 40 year objective climatology of surface cyclones in the Mediterranean region: spatial and temporal distribution, International Journal of Climatology, 10.1002/joc.599, 21, 1, (109-130).
33. Nielsen, J. W., and R. M. Dole, 1992: A survey of extratropical cyclone characteristics during GALE. Mon. Wea. Rev., 120, 1156–1167.
34. Pinto, J.G., Spangeh, T., Ulbrich, U., Speth, P., 2005. Sensitivities of a cyclone detection and tracking algorithm: individual tracks and climatology. Meteorol. Z. 14, 823–838.
35. Prezerakos NG. 1985. The northwest African depressions affecting the south Balkans. Journal of Climatology 5: 643–654.
36. Prezerakos NG, Michaelides SC, Vlassi AS (1990) Atmospheric synoptic conditions associated with the initiation of north-west African depressions. Int J Climatol 10:711–729.
37. Prospero, J.M., Ginoux, P., Torres, O., Nicholson, S.E., Gill, T.E., 2002. Environmental characterization of global source of atmospheric soil dust identified with the Nimbus 7 Total Ozone Mapping Spectrometer (TOMS) absorbing aerosol product. Rev. Geophys. 40 (1), 1002. doi:10.1029/2000RG000095.
38. Raible, C. C., and R. Blender, 2004: Northern Hemisphere midlatitude cyclone variability in GCM simulations with different ocean representations. Climate Dyn., 22, 239–248.
39. Raible CC, Della-Marta P, Schwierz C, Wernli H, Blender R (2008) Northern Hemisphere extratropical cyclones: a comparison of detection and tracking methods and different re-analyses. Mon Weather Rev 136:880–897.

40. Romem M, Ziv B, Saaroni, H (2007) Scenarios in the development of Mediterranean cyclones. Adv Geosci 12:59–65. doi:10.5194/adgeo-12–59–2007.
41. Rubin S, Ziv B, Paldor N (2007) Tropical plumes over eastern North Africa as a source of rain in the Middle East. Mon Weather Rev 35(12):4135–4148
42. Schubert, M., J. Perlwitz, R. Blender, K. Fraedrich, and F. Lunkeit, 1998: North Atlantic cyclones in CO2-induced warm climate simulations: Frequency, intensity, and tracks. Climate Dyn., 14, 827–838.
43. Simmons, A. J., and G. Watterson, 1999: Objective assessment of extratropical
44. weather systems in simulated climates. J. Climate, 12, 3467–3485.
45. Sokolik, I. N., D. M. Winker, G. Bergametti, D. A. Gillette, G. Carmichael, Y. Kaufman, L. Gomes, L. Schuetz, and J. E. Penner, Introduction to special section: Outstanding problems in quantifying the radiative impacts of mineral dust, J. Geophys. Res., 106, 18,015–18,028, 2001.
46. Tantawy, A. H. I., On the cyclogenesis an structure of spring Sahara depressions in subtropical Africa, Meteorol. Res. Bull., 69, pp. 68-107, Dep. of Meteorol., United Arab Republic, Cairo, 1969.
47. Tegen, I., P. Hollrig, M. Chin, I. Fung, D. Jacob, and J. Penner, Contribution of different aerosol species to the global aerosol extinction optical thickness: Estimates from model results, J. Geophys. Res., 102, 23,895–23,916, 1997.
48. Thorncroft C, Flocas H (1997) A case study of Saharan cyclogenesis. Mon Wea Rev 125(6):1147–1165
49. Trigo IF, Davies TD, Bigg GR (1999) Objective climatology of cyclones in the Mediterranean region. J Climate 12(6):1685–1696
50. Trigo IF, Bigg GR, Davies TD (2002) Climatology of cyclogenesis mechanisms in the Mediterranean. Mon Weather Rev 130:549–569.
51. Trigo IF (2006) Climatology and interannual variability of stormtracks in the Euro-Atlantic sector: a comparison between ERA-40 and NCEP/NCAR reanalyses. Clim Dyn 26:127–143
52. Varga, G., Újv´ari, G., Kov´acks, J., 2014. Spatiotemporal patterns of saharan dust outbreaks in the mediterranean basin. Aeolian Res. 15, 151–160. https://doi.org/10.1016/j.aeolia.2014.06.005.
53. Wang XL, Swail VR, Zwiers FW (2006) Climatology and changes of extratropical cyclone activity: comparison of ERA-40 with NCEP-NCAR reanalysis for 1958–2001. J Clim 19:3145–3166.
54. Wernli, H., and C. Schwierz, 2006: Surface cyclones in the ERA-40 data set (1958–2001). Part I: Novel identification method and global climatology. J. Atmos. Sci., 63, 2486–2507.

Figures

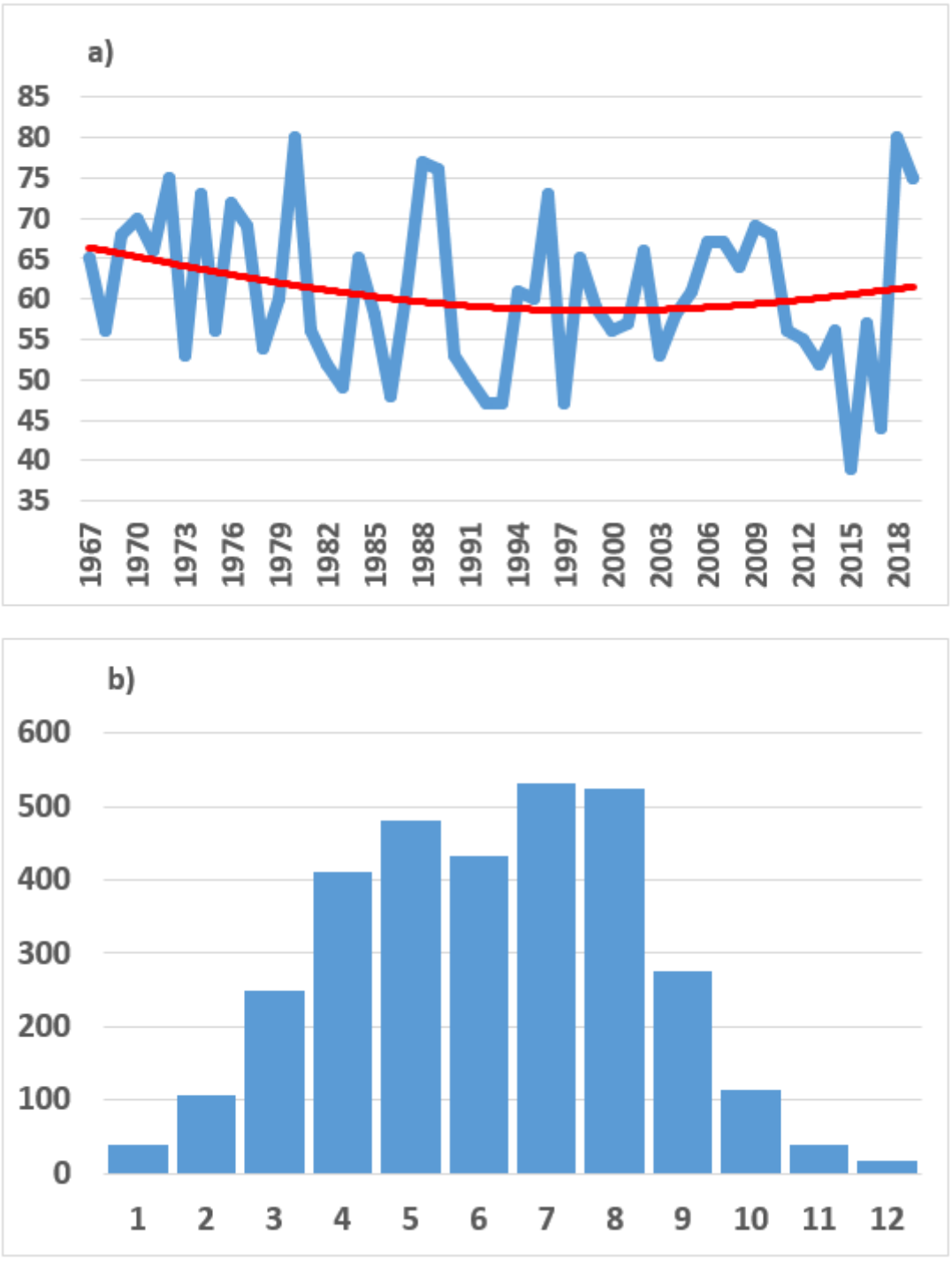

Figure 1

a) The annual time series of all detected long-track cyclones (blue line) and their annual trend (red line) and b) the monthly distribution of detected long-track cyclones for the period from 1967-2019

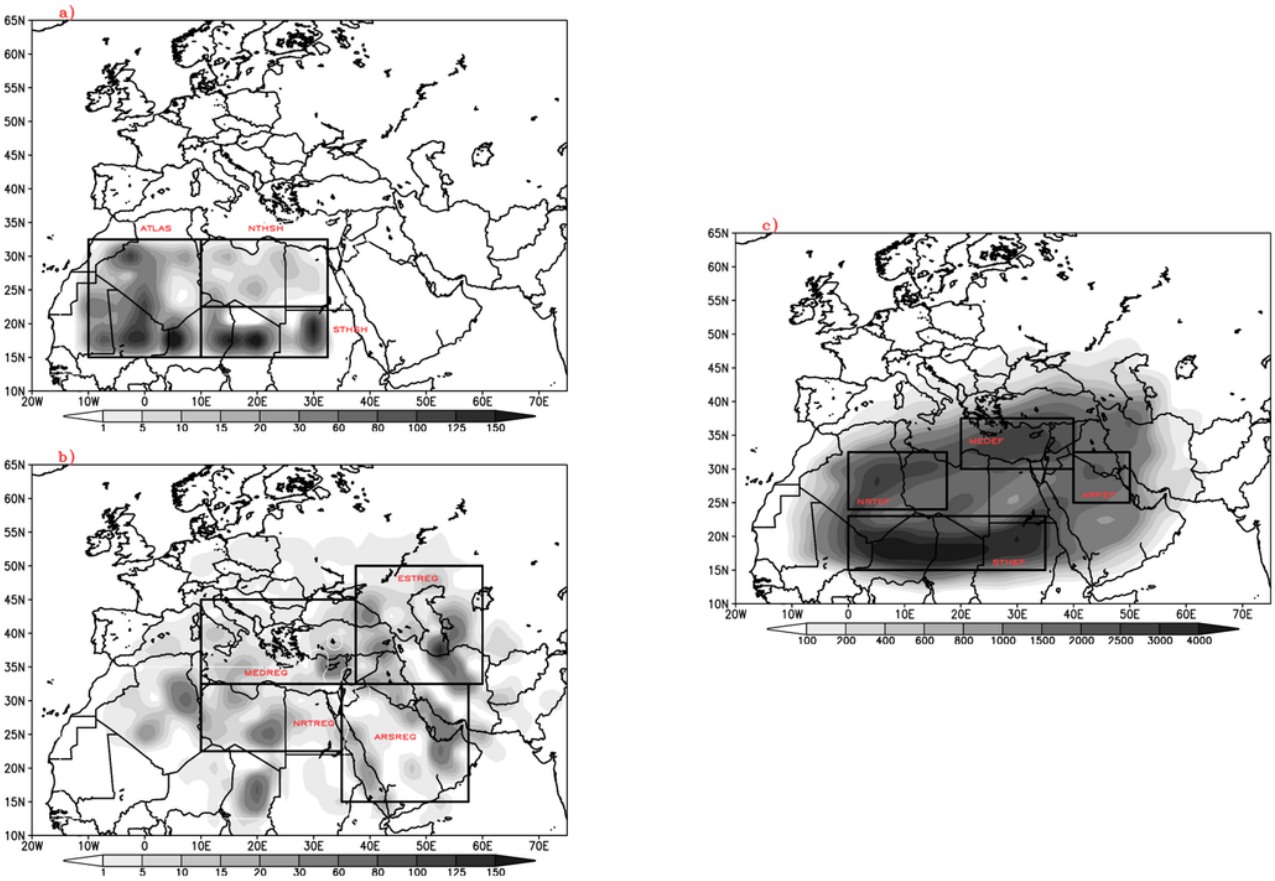

Figure 2

a) Cyclogenesis areas over the Saharan region for detected long-track cyclones from 1967-2019. In the figure, “ATLAS”, “NTHSH” and “STHSH” mean Atlas, North Sahara and South Sahara areas, respectively. b) Cyclolysis areas of the long-track cyclones from 1967-2019. In the figure, “MEDREG”, “NRTREG”, “ARSREG” and “ESTREG” mean Mediterranean, North African, Arabian Peninsula and Red Sea and Eastern areas, respectively. c) The areas most affected by the detected long-track cyclones from 1967-2019; in the figure, “STHEF”, “NRTEF”, “METEF” and “ARPEF” represent the South Sahara, North Sahara, Mediterranean and Arabian Peninsula effective regions, respectively.

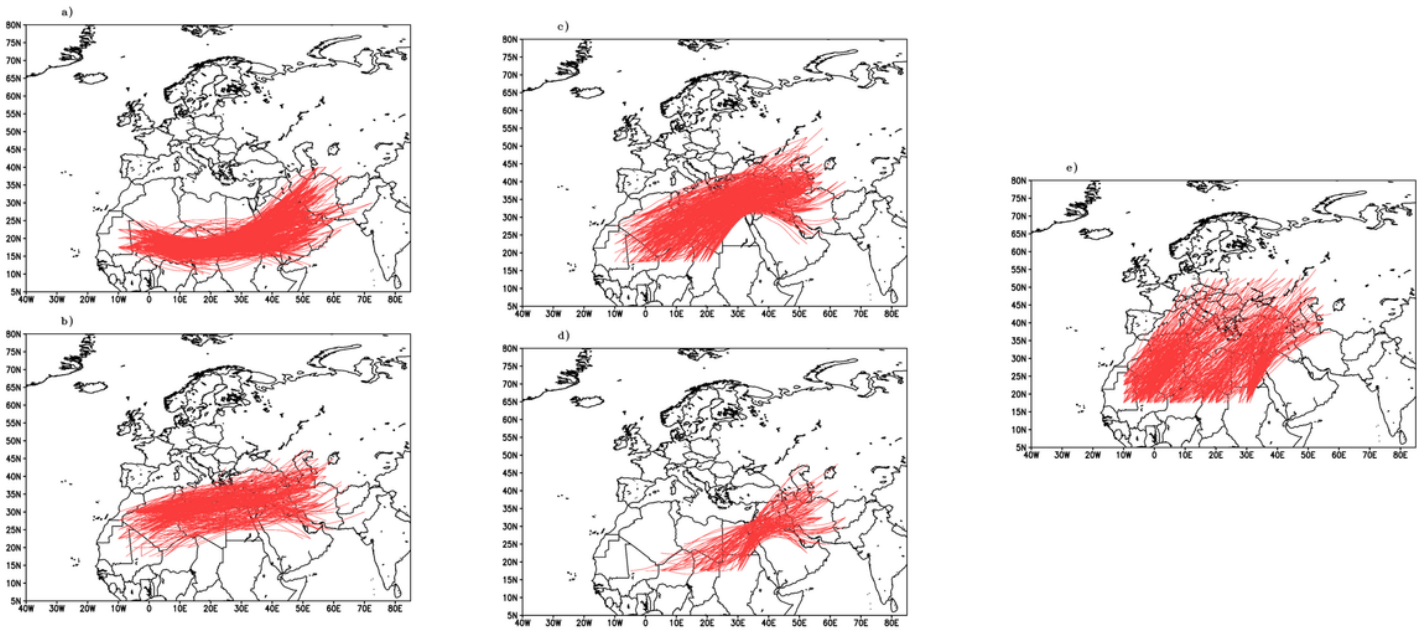

Figure 3

Identified cyclone track routes: (a) South Sahara route, (b) North Sahara route, (c) Eastern Mediterranean route, (d) Northeast Egypt route and (e) Northern route

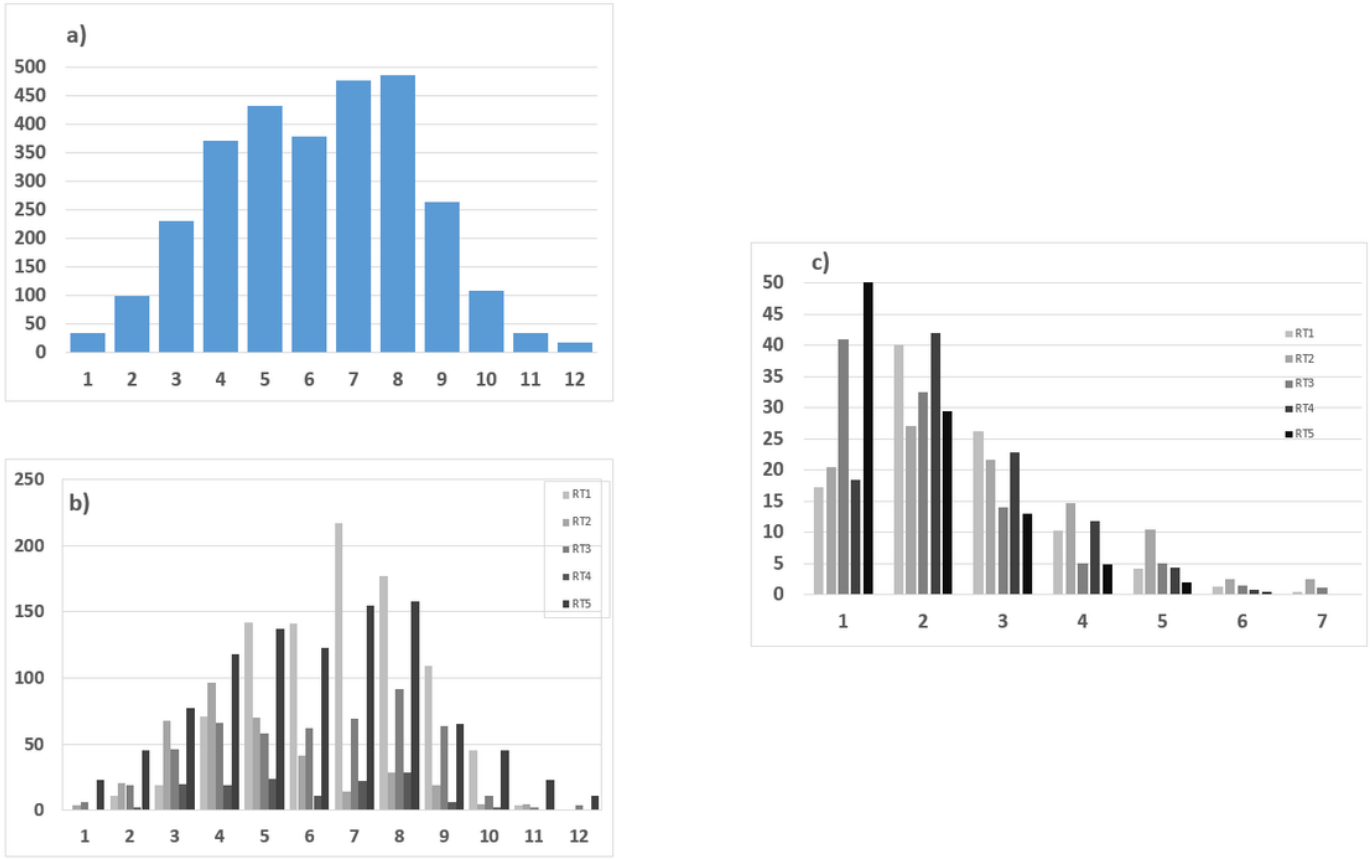

Figure 4

a) Monthly distribution of the number of classified cyclone tracks along the main routes; b) monthly distribution of each classified cyclone track type along the main routes and c) daily lifespan of each classified track along the main routes from 1967-2019

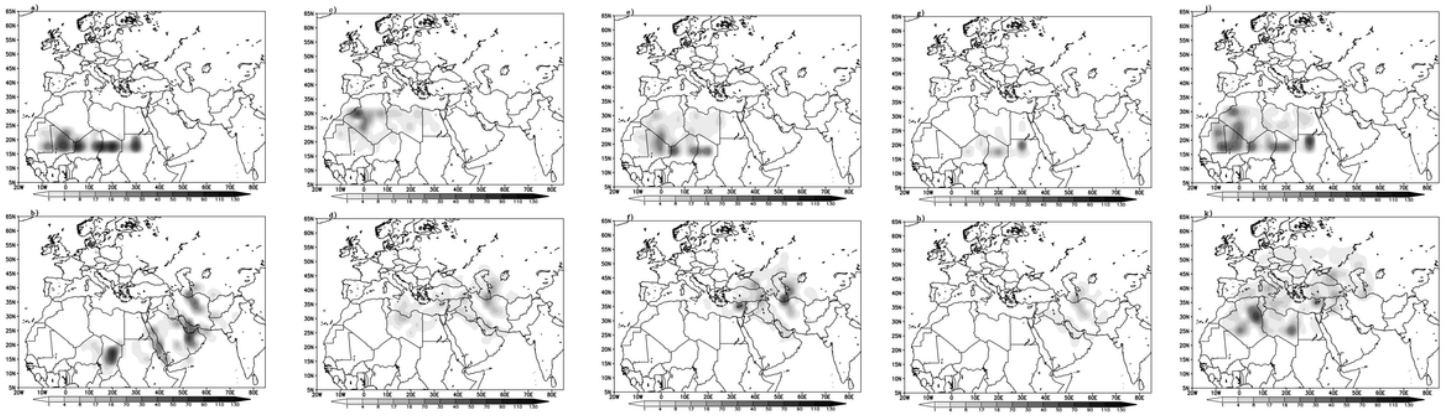

Figure 5

The cyclogenesis areas for the (a) South Sahara route, (c) North Sahara route, (e) Eastern Mediterranean route, (g) Northeast Egypt route and (j) Northern route and the cyclolysis areas for the b) South Sahara route, (d) North Sahara route, (f) Eastern Mediterranean route, (h) Northeast Egypt route and (k) Northern route